Long distance stability of gap solitons

T. Richter, K. Motzek, and F. Kaiser
Institute of Applied Physics, Darmstadt University of Technology, Hochschulstrasse 4a, D-64289 Darmstadt, Germany
(Received 31 August 2006; published 2 January 2007)

We numerically investigate the stability of one- and two-dimensional gap solitons for very long propagation distances both in self-focusing and in self-defocusing nonlinear photonic media. We demonstrate that the existence of stable solitons in the first gap requires much stronger lattices in a self-focusing than in a self-defocusing medium. Moreover, we present a one-dimensional linear stability analysis of the fundamental solitary mode in the first gap considering a self-focusing photorefractive nonlinearity.

DOI: 10.1103/PhysRevE.75.016601 PACS number(s): 42.65.Tg, 42.65.Jx, 42.65.Wi

I. INTRODUCTION

During the last years, much attention in nonlinear optics has been focused on periodic structures such as photonic crystals [1]. These systems are known to allow linear wave propagation only if the corresponding wave vectors lie within certain intervals, the so-called Bloch bands. However, nonlinear photonic media support spatially localized structures—usually termed gap solitons—whose wave vectors lie in the gaps between the Bloch bands. Gap solitons may occur in very different physical systems such as fiber Bragg gratings [2], waveguide arrays [3,4], Bose-Einstein condensates in optical lattices [5,6], and optically induced photonic lattices [7–9].

There have been several publications in the past regarding the stability properties of different kinds of gap solitons, both purely numerical [10] and combined numerical and analytical [11] ones. These studies reveal a deeper connection between instabilities and resonances in the Bloch bands caused by the internal modes of the solitons. However, they consider only a fixed value for the strength of the photonic lattice. In this paper we investigate the dependency of the soliton stability on the lattice strength, comparing self-focusing and self-defocusing nonlinearities. Additionally, we show that similar instabilities exist in transversally two-dimensional systems. We choose a photonic crystal with a saturable, photorefractive nonlinearity as model system. Our results are applicable—at least qualitatively—to Kerr-type nonlinearities as well, thus they may be transferred to any system that can be described by a (modified) nonlinear Schrödinger equation with a periodic potential, such as Bose-Einstein condensates in optical lattices.

This paper is organized as follows: After a short description of our model in Sec. II, we perform a one-dimensional (1D) linear stability analysis (Sec. III) and show that there are no stable self-focusing solitons in the first gap for moderate lattice strengths. After that, we carry out detailed numerical simulations for both focusing and defocusing nonlinearities. In Sec. IV we transfer our results to transversally two-dimensional systems.

II. MODEL

The propapagtion of a light beam through a nonlinear photonic crystal can be described in two transverse dimensions by the following equation for its slowly varying envelope $A(x,y,z)$:

$$\partial_z A = \frac{i}{2}[\nabla_\perp^2 + V_m(x,y)]A - \sigma\frac{i}{2}\gamma E_{nl}(|A|^2)A. \tag{1}$$

Herein $V_m(x,y)$ denotes the static modulation of the refractive index (photonic lattice), γ is the nonlinear coupling constant, and $\nabla_\perp^2 = \partial_{xx} + \partial_{yy}$ is the transverse Laplacian. The sign factor σ has been introduced to determine the character of the nonlinearity: $\sigma = +1$ describes a self-defocusing and $\sigma = -1$ is a self-focusing medium if $E_{nl} > 0$. Equation (1) has been made dimensionless by introducing a transversal (x and y directions) scaling constant w_0 and a longitudinal (z direction) scaling constant $z_0 = kw_0^2$ (k being the wave vector in the unperturbed and unmodulated medium). All numerical simulations in this paper are carried out with $\gamma = 30$, and we consider the continuous, separable modulation

$$V_m(x,y) = V_0 \cdot [\cos^2(\pi/d \cdot x) + \cos^2(\pi/d \cdot y)] \tag{2}$$

with the modulation depth V_0 and the grid constant d. We use $d = 2w_0$ in all of our simulations.

Solitary solutions can be obtained by inserting the soliton condition $A(x,y,z) = a(x,y)\cdot\exp(i\beta z)$ into Eq. (1); this yields the relation

$$[2\beta - \nabla_\perp^2 - V_m(x,y)]a + \sigma\gamma E_{nl}(|a|^2)a = 0 \tag{3}$$

which contains the propagation constant β. Since we are considering slowly varying envelopes, this parameter constitutes an offset to the wave vector in the propagation direction.

There are several ways of modeling the nonlinearity (i.e., the electric screening field) $E_{nl}(|A|^2)$ of a photorefractive crystal. The most appropriate one is to derive an expression for its scalar potential ϕ directly from Kukhtarev's model using some well-justified simplifications [12]. Neglecting diffusion effects this leads to

$$\nabla[(1 + |A|^2)\nabla\phi] = -\partial_x|A|^2, \quad E_{nl} = -\partial_x\phi. \tag{4}$$

Due to the single partial x derivative on the right hand side Eqs. (4) describe an anisotropic nonlinearity. In the transversally one-dimensional case they can be reduced to

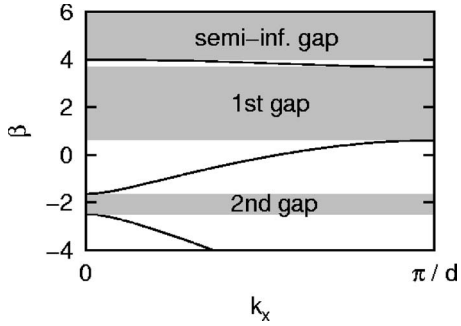

FIG. 1. Dispersion relation for the 1D photonic lattice.

$$E_{nl} = |A|^2/(1+|A|^2). \tag{5}$$

We carry out our 1D simulations using Eq. (5) and our 2D simulations using Eq. (4); however, our results do not crucially depend on the exact shape of the nonlinearity.

III. 1D SIMULATIONS

Figure 1 shows the dispersion relation of the Bloch waves in a 1D photonic lattice; the corresponding modulation potential simply reads $V_m(x)=V_0\cdot\cos^2(\pi/d\cdot x)$ [cf. Eq. (2)]. A superposition of Bloch waves forms a soliton only if the nonlinearity of the medium can compensate the curvature of the dispersion relation. The sign of this curvature changes within each band, so this can be achieved both for defocusing (solitons bifurcate from the lower band edges) and for focusing (solitons bifurcate from the upper band edges) nonlinearities. Therefore only in the latter case can solitons exist in the semi-infinite gap. Since these are nodeless, their stability can be proven analytically using the Vakhitov-Kolokolov criterion [13].

Investigating the stability of solitons within the other band gaps is more complicated. First we perform a linear stability analysis by considering the evolution of a perturbed solitary solution $a(x)$ [11],

$$A(x,z) = e^{i\beta z}(a(x) + \varepsilon\{[v(x)+iw(x)]e^{\lambda z} + [v(x)^* + iw(x)^*]e^{\lambda^* z}\}). \tag{6}$$

The corresponding eigenvalue problem reads

$$\lambda v = -\mathcal{L}w,$$

$$\lambda\omega = \mathcal{L}v - \sigma\gamma\partial_I E_{nl}(I)a^2 v, \quad I = |a|^2 \tag{7}$$

with

$$\mathcal{L} \equiv -\beta + \frac{1}{2}\nabla_\perp^2 + \frac{1}{2}V_m(x) - \frac{1}{2}\sigma\gamma E_{nl}(|a|^2). \tag{8}$$

In general Eq. (7) can be solved only numerically and by using large grids since the eigenmodes have very long oscillating tails. We start with a self-focusing fundamental solitary mode in the first gap and a medium lattice strength; the results are shown in Fig. 2. There are three dominating eigenmodes, a single-peaked symmetric one [mode I, Fig. 2(b)] and both a symmetric and an antisymmetric double-peaked one [modes II and III, Figs. 2(c) and 2(d)]. Each of them may become unstable within one or more intervals [Fig. 2(a)], and the union of these intervals covers the complete first gap.

Therefore these results suggest that in this case there are no stable solitons at all, but we should bear in mind that the numerical accuracy of our stability analysis may become poor within regions of very weak instabilities [i.e., $\mathrm{Re}(\lambda) \ll 1$], which we obtain, e.g., around $\beta=2$. This is due to the special symmetry of Eq. (7): The two eigenvalue equations can be rewritten as a single one containing only λ^2, and thus each eigenmode with $\mathrm{Re}(\lambda)\neq 0$ is actually linearly unstable since it occurs twice, and once with $\mathrm{Re}(\lambda)>0$. Hence we have to distinguish these modes from linearly neutrally

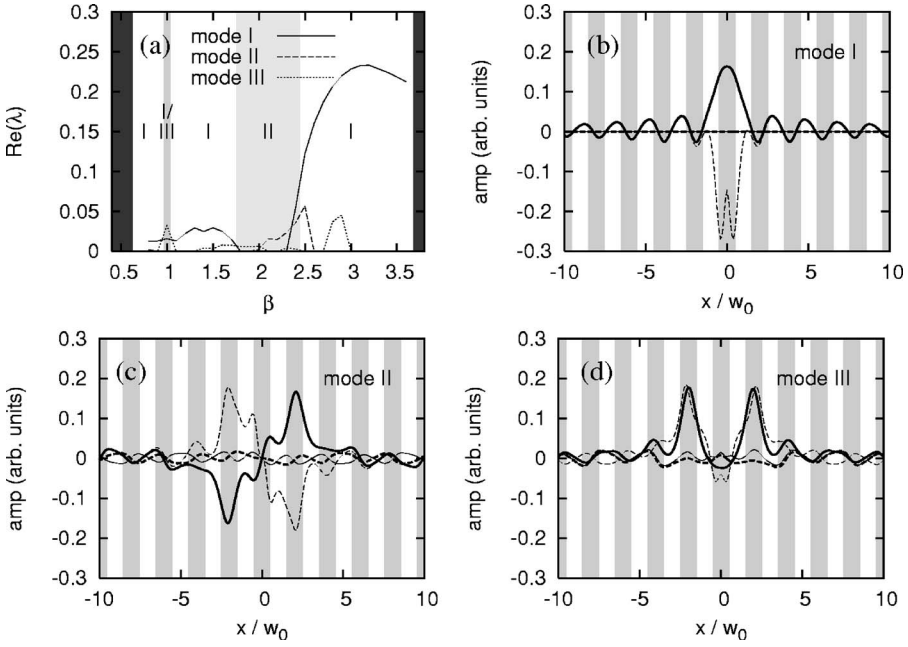

FIG. 2. Linear stability analysis of the fundamental self-focusing ($\sigma=-1$) solitary mode in the first gap ($V_0=13.6$): (a) real parts of the eigenvalues for the three dominating unstable eigenmodes; the numbers in the shaded bars indicate the modes which cause the decay of the soliton in the numerical simulations; (b)–(d) real (—) and imaginary (--) parts of v (thick lines) and w (thin lines) for the modes from (a); gray bars in (b)–(d) indicate regions with a high static refractive index.

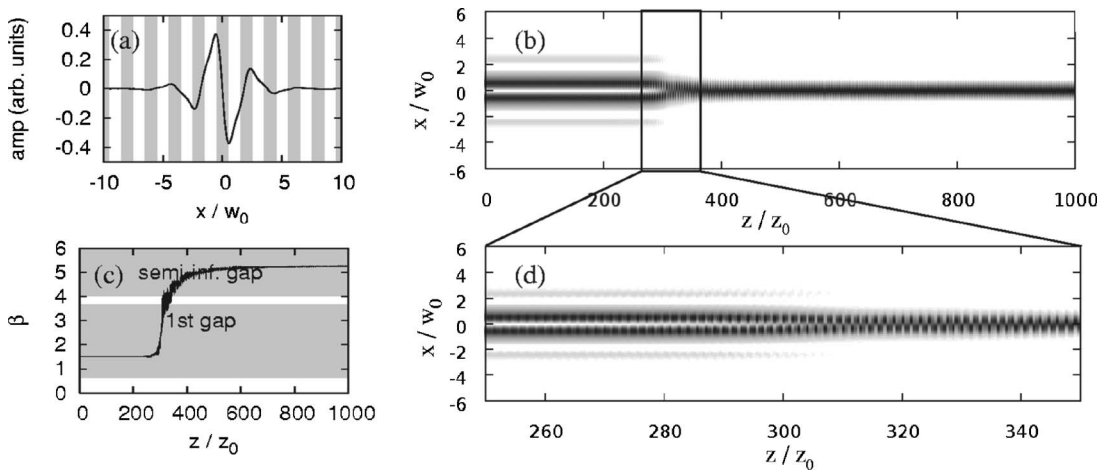

FIG. 3. Decay of the fundamental self-focusing ($\sigma=-1$) solitary mode with $\beta=1.5$ (first gap) and $V_0=13.6$ due to the symmetric eigenmode from Fig. 2(b): (a) soliton profile, gray bars indicate regions with a high static refractive index; (b) intensity distribution over the propagation distance; (c) spatial evolution of the mean propagation constant; (d) detailed view of the decay. Dark gray tones in (b) and (d) indicate high intensities.

stable ones, and this becomes difficult if Re(λ) is small.

Thus we try to verify these results by propagating the corresponding solitary solutions numerically over sufficiently large distances. In order to do this we need a propagation algorithm that is both fast and capable of handling absorbing boundary conditions since otherwise artificial reflections occurring at the grid boundaries might obscure the soliton decays. We therefore use the technique of perfectly matched layers (PMLs) [14] in combination with a Hopscotch integration scheme applied to Eq. (1) in all of our simulations.

The results of the simulations are shown in Figs. 3 and 4. The qualitative agreement between the unstable domains determined from the simulations [shaded bars in Fig. 2(a)] and those determined from the linear stability analysis is quite good, smaller deviations occur especially when several modes with $0<\mathrm{Re}(\lambda)\ll 1$ compete. In these cases the accuracy of the simulations is usually higher due to the reasons mentioned above.

As Fig. 2(a) already suggests, mode I from Fig. 2(b) governs the soliton decay for $\beta\lesssim 1.7$ (Fig. 3) and $\beta\gtrsim 2.5$, while mode II [Fig. 2(c)] dominates for $1.7\lesssim\beta\lesssim 2.5$ (Fig. 4), even if the latter does not seem to be clear from the stability analysis alone. In contrast to the stability analysis the simulations unveil only a very small interval around $\beta=1$ where the influence of mode III becomes significant, and even there it is comparable to that of the single-peaked symmetric mode.

The propagation constant of the original soliton shifts during the decay from the first towards the semi-infinite band gap, and the intensity profile converges against a stable fundamental soliton having some internal modes excited [Figs. 3(c) and 4(c), respectively]. Considerable amounts of intensity are radiated by the beam only during the change of β.

Corresponding to the higher values of Re(λ) the instability caused by mode I sets in faster than the one caused by mode II. Since mode I is symmetric, this instability is symmetry breaking, what can be seen clearly from the alternating intensity oscillations [Figs. 3(b) and 3(d)]. The spatial ampli-

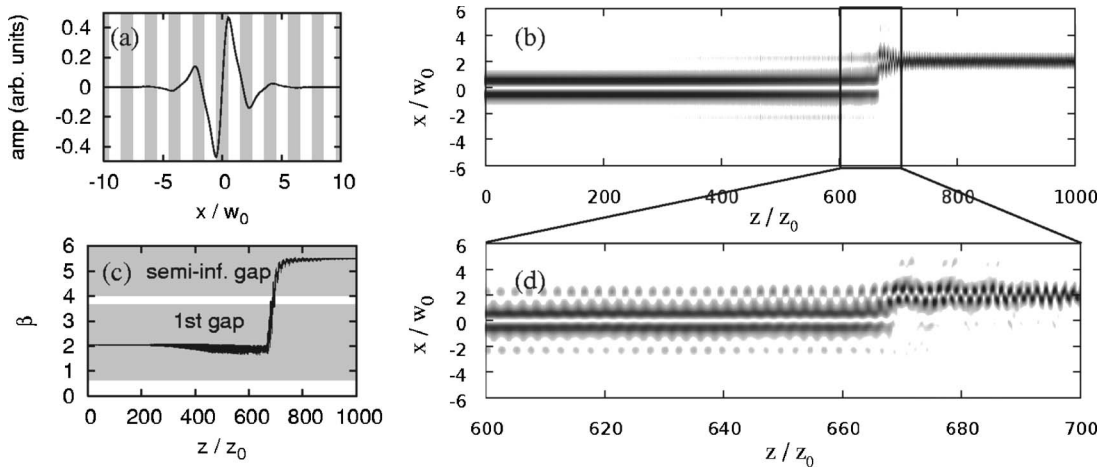

FIG. 4. Decay of the fundamental self-focusing ($\sigma=-1$) solitary mode with $\beta=2$ (first gap) and $V_0=13.6$ due to the antisymmetric eigenmode from Fig. 2(c); the meaning of (a)–(d) is the same as in Fig. 3.

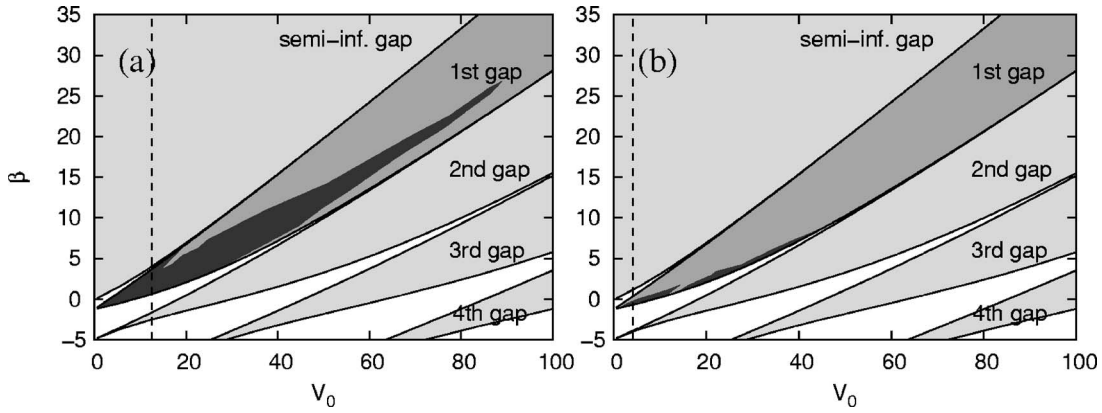

FIG. 5. Stability vs lattice depth ($d=2$) for fundamental solitons in the first gap: (a) self-focusing, (b) self-defocusing nonlinearity. Shadings: light gray, band gaps; medium gray, stable regions (first gap); dark gray, unstable regions (first gap). Dashed lines: potential depths from (a) Figs. 2–4 and (b) Fig. 6, respectively.

tude of these oscillations decreases during the decay ($300z_0 \lesssim z \lesssim 400z_0$), what finally leads to a slightly oscillating fundamental solitary mode in the semi-infinate gap, as mentioned above. Except for these oscillations, the final structure is centred around the origin at $x=0$. For $\beta \gtrsim 2.5$ the decay of these oscillations may last very long, despite the large growth rate of the initial instability corresponding to Re(λ).

The values of Re(λ) for the double-peaked antisymmetric mode II are very small, therefore the propagation distances which are necessary to observe the corresponding instability may be large [Figs. 4(b) and 4(d)]. The instability is symmetry-conserving until the mode from Fig. 2(d) becomes also excited ($z \approx 665z_0$), causing a shift of the center of intensity. This shift finally leads to a sudden jump ($z \approx 670z_0$) of the major part of the beam into the neighboring static waveguide of the photonic lattice (in Fig. 4 it is the one at $x=+2w_0$, but the jump could occur in the opposite direction as well). Again we have an oscillating fundamental mode at the end, propagating in the semi-infinite gap.

As it has been shown in [11], the instabilities we observe here conincide with resonances in the Bloch bands, which may occur when at least one of the sidebands $\beta \pm \mathrm{Im}(\lambda)$ of an internal mode obtained from Eq. (7) lies within a Bloch band. Since the Bloch bands become narrower the stronger the photonic lattice is, it seems to be obvious that gap solitons should become stable if the depth of the lattice is high enough. In order to investigate this in detail, we repeat our stability analysis and our simulations for different lattice depths V_0. We do not have to vary the lattice constant d, since the propagation equation (1) can be scaled in such a way that this is equivalent to changing V_0.

The result of this analysis for the self-focusing nonlinearity is shown in Fig. 5(a). For $V_0 \lesssim 13.8$ all solitons in the first gap are unstable. For greater values of V_0, the solitons with a high total intensity (i.e., those lying close to the upper egde

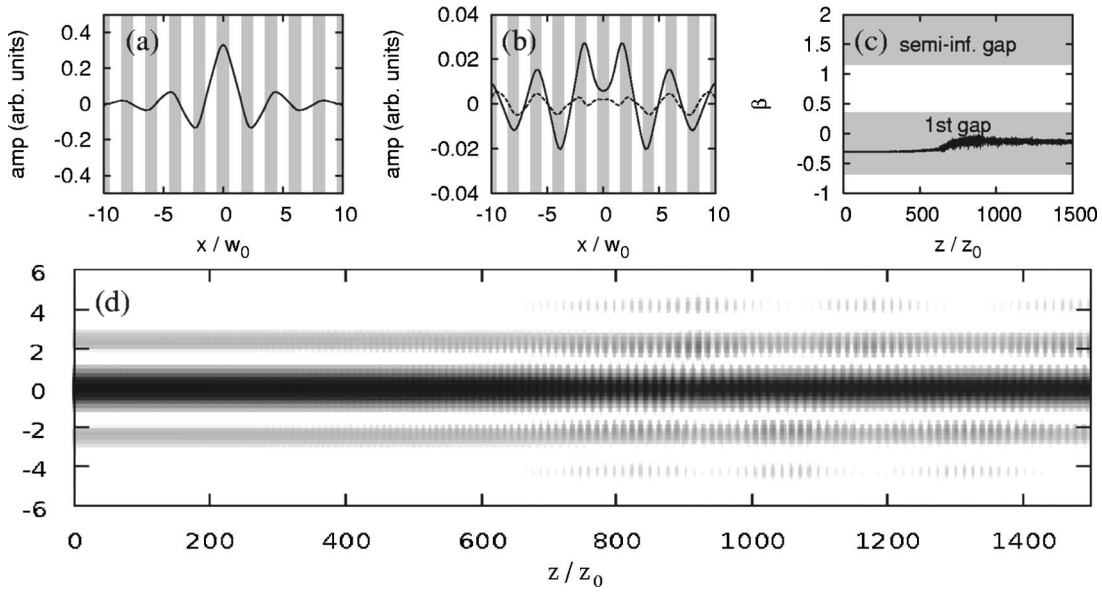

FIG. 6. Decay of the fundamental self-defocusing ($\sigma=1$) solitary mode with $\beta=-0.3$ (first gap) and $V_0=4.2$: (a) soliton profile, gray bars indicate regions with a high static refractive index; (b) real (—) and imaginary (- -) part of the dominating unstable eigenmode; (c) spatial evolution of the mean propagation constant; (d) view of the decay. Dark gray tones in (d) indicate high intensities.

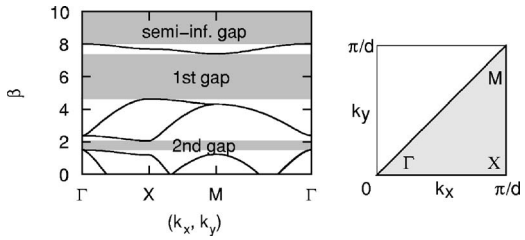

FIG. 7. Dispersion relation (left) and irreducible part of the first Brillouin zone (right) for the 2D photonic lattice corresponding to Eq. (2).

of the gap) become stable; for $V_0 \gtrsim 28$ those with a low total intensity become stable as well. The unstable region finally ends at $V_0 \approx 90$, where also the third Bloch band has become small. This leads to the conclusion that Bloch bands of higher than third order do not play an important role for soliton instabilities in the first gap.

For the largest part of the unstable region in Fig. 5(a), the soliton decays are ruled by eigenmodes of type I from Fig. 2. The other modes become important mainly in a certain interval around the dashed line (i.e., approximately for $V_0 = 13.6 \pm 5$).

Interestingly enough the situation is completely different if one carries out the same analysis for a self-defocusing medium [Fig. 5(b)]. Here we observe stable solitons down to very weak lattices ($V_0 \approx 1.5$ and lower). Instabilities occur only in a small range near the lower gap edge (i.e., for solitons with a high total intensity). They finally disappear for $V_0 \gtrsim 45$, when the second Bloch band has become small. In contrast to the self-focusing case the unstable regions are very small, and resonances within the third band do not seem to occur.

Figure 6 shows the decay of an unstable self-defocusing soliton with $\beta = -0.3$ and $V_0 = 4.2$. We choose a different potential strength here than in Figs. 3 and 4, since otherwise the instabilities are very weak. The dominating unstable eigenmode is symmetric and leads to an oscillation of the soliton, but—in contrast to the self-focusing case—its structure is not destroyed. The propagation constant remains in the first gap, but it is shifted into the stable regime.

Although we do not discuss the stability of solitons in higher order gaps in detail here, we mention that there are

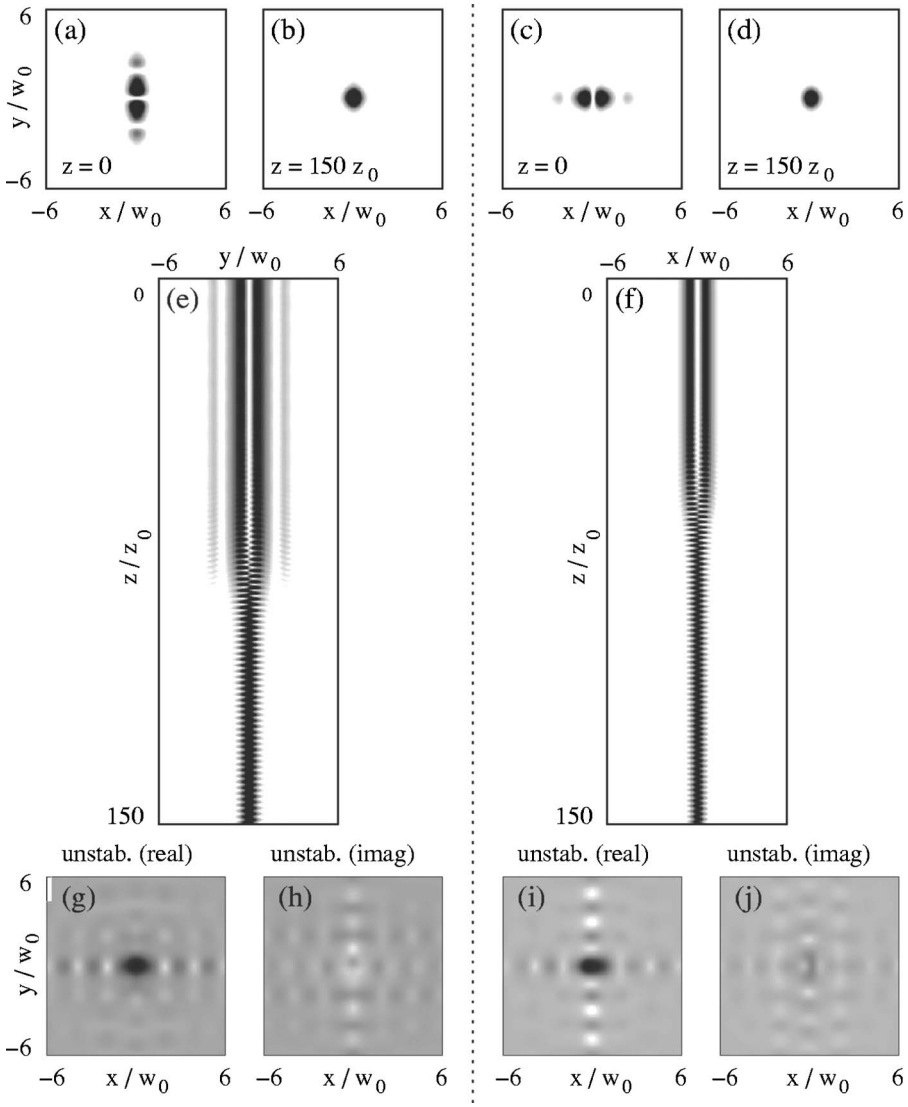

FIG. 8. Decay of the two fundamental 2D self-focusing ($\sigma = -1$) solitary modes with $\beta = 5.5$ (first gap) and $V_0 = 27.2$ for the anisotropic photorefractive nonlinearity. Top: intensity profiles before [(a), (c)] and after [(b), (d)] the decay; middle: cross sections [(e) y-z plane and (f) x-z plane, respectively]; bottom: real [(g), (i)] and imaginary [(h), (j)] parts of the dominating unstable eigenmodes. Dark gray tones indicate high intensities (a)–(f) or high amplitudes (g)–(j), respectively.

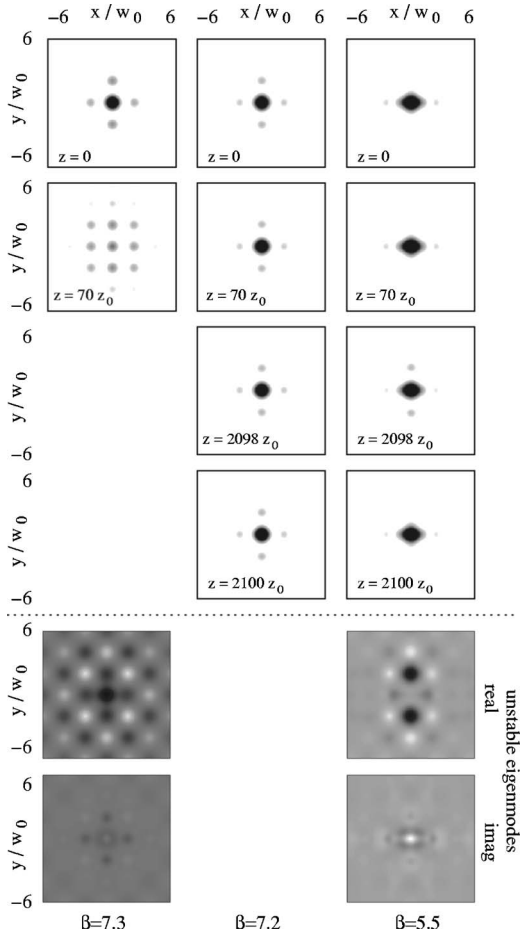

FIG. 9. Upper part: propagation of the 2D fundamental defocusing ($\sigma=1$) solitary mode for three different values of β (7.3, 7.2, and 5.5) in the first gap ($V_0=27.2$) for the anisotropic photorefractive nonlinearity; lower part: dominating unstable eigenmodes. The mode shown in the middle column is stable. Dark gray tones indicate high intensities (upper part) or high amplitudes (lower part), respectively.

much higher lattice depths necessary in order to stabilize them. If they are unstable, the decay is similar to the one of first-gap solitons in that sense, that it also ends up with a stable, slightly oscillating fundamental mode in the lowest-possible gap (i.e., the semi-infinite one for self-focusing and the first one for self-defocusing nonlinearities).

The value of the nonlinear coupling constant γ does not seem to have a crucial influence on our results (as long as it is not too small). The same holds for the concrete form of the nonlinearity given by Eq. (5); we obtain comparable results for media with a Kerr nonlinearity [$E_{nl}(|a|^2) \propto |a|^2$].

Because of the latter fact there is a close relation between the system discussed here and Bose-Einstein condensates in optical lattices (cf. [10,11]), since the propagation equation (1) with a Kerr nonlinearity is formally equivalent to the Gross-Pitaevskii equation when one reinterprets the propagation in the z direction as temporal evolution.

IV. 2D SIMULATIONS

We now investigate how far these results may change when we consider two transverse dimensions. Figure 7 shows the dispersion relation and the irreducible part of the first Brillouin zone for the corresponding 2D photonic lattice as it is given by Eq. (2).

At first we again consider the fundamental self-focusing solitary modes in the first gap. As it can be seen from the Figs. 8(a) and 8(c), their shape is just the simplest possible, spatially localized 2D extension of the corresponding 1D modes. As a consequence of the anisotropy of our model, we now have to distinguish between two orientations (horizontal and vertical) of the solitons. Figure 8 shows that also in this case a slowly growing instability corresponding to a single-peaked symmetric unstable eigenmode exists. Consequently, when viewed in the y-z or x-z plane, respectively [Figs. 8(e) and 8(f)], the decay has many similarities with Fig. 3(b). It also starts with a slowly increasing, alternating pulsing due to the symmetry breaking and ends up with a slightly oscillating fundamental solitary mode in the semi-infinite gap [Figs. 8(b) and 8(d)]. This kind of decay is the only one which we observe for the 2D system. Again, the solitons become stable for very strong lattices (factor $2\cdots5$ stronger than in Fig. 8).

The vertically oriented mode has a slightly lower total intensity than the horizontally oriented one, and the decay sets in a little later. We observe this "correlation" between total intensity and the growth rate of the instability in many of our 2D simulations. It also exists in the 1D case when the fundamental, symmetric unstable eigenmode (mode I from Fig. 2) dominates over the complete first gap.

Like in the 1D system, self-defocusing solitons may be stable for much weaker lattices than self-focusing ones. When we use the same lattice strength as in Fig. 8, we observe instabilities only for very low (left column of Fig. 9) and for very high (right column of Fig. 9) soliton instensities. The latter are already known to us from the 1D case (cf. Fig. 6): the structure of the soliton is not destroyed but starts to oscillate, and the propagation constant is shifted towards the stable region. Due to the anisotropy of our model the oscillation takes place in the y direction, i.e., the upper and the lower spot appear and disappear periodically (cf. the pictures at $z=2098z_0$ and $z=2100z_0$ in the right column of Fig. 9). Consequently, the real part of the corresponding unstable eigenmode has two maxima at $y=\pm 2w_0$.

However, the instability near the upper egde of the first gap (left column of Fig. 9) seems to occur only in the 2D case. In contrast to all other instabilities we discussed in this paper, it is of a nonoscillatory type and it does not lead to the formation of a new, stable soliton; the beam rather diffracts strongly after a certain propagation distance. A slight increment of the soliton intensity (that means, raising the propagation constant a little) is sufficient to stabilize the structure, as shown in the middle column of Fig. 9.

V. CONCLUSIONS

In this paper we presented a numerical investigation of the stability properties of gap solitons, whereas we considered the first gap in detail. We compared self-focusing and self-defocusing nonlinearities and we demonstrated that in

the former case gap solitons are subject to slowly growing oscillatory instabilities unless the photonic lattice is very strong. These instabilities lead to a complete decay of the original solitons, and a slightly oscillating, stable fundamental mode in the semi-infinite gap remains.

We also obtained oscillatory instabilities for self-defocusing solitons, but in the first gap the corresponding regimes are only marginal in the parameter space. The structure of the solitons is not destroyed, but starts to oscillate, and the propagation constant is shifted towards the stable regime.

We found that these results hold qualitatively both for 1D and for 2D systems, and they are not limited to photorefractive nonlinearities. Solitons in higher order gaps are also subject to oscillatory instabilities, and their decay usually leads to a stable, slightly oscillating fundamental mode in the lowest-possible gap (i.e., the semi-infinite one for focusing and the first one for defocusing nonlinearities).

[1] Y. S. Kivshar and G. P. Agrawal, *Optical Solitons: From Fibers to Photonic Crystals* (Academic, San Diego, 2003).
[2] B. J. Eggleton, R. E. Slusher, C. M. de Sterke, P. A. Krug, and J. E. Sipe, Phys. Rev. Lett. **76**, 1627 (1996).
[3] D. Mandelik, H. S. Eisenberg, Y. Silberberg, R. Morandotti, and J. S. Aitchison, Phys. Rev. Lett. **90**, 053902 (2003).
[4] D. Mandelik, R. Morandotti, J. S. Aitchison, and Y. Silberberg, Phys. Rev. Lett. **92**, 093904 (2004).
[5] E. A. Ostrovskaya and Y. S. Kivshar, Phys. Rev. Lett. **90**, 160407 (2003).
[6] B. B. Baizakov, V. V. Konotop, and M. Salerno, J. Phys. B **35**, 5105 (2002).
[7] J. W. Fleischer, M. Segev, N. K. Efremidis, and D. N. Christodoulides, Nature (London) **422**, 147 (2003).
[8] J. W. Fleischer, T. Carmon, M. Segev, N. K. Efremidis, and D. N. Christodoulides, Phys. Rev. Lett. **90**, 023902 (2003).
[9] R. Fischer, D. Träger, D. N. Neshev, A. A. Sukhorukov, W. Krolikowski, C. Denz, and Y. S. Kivshar, Phys. Rev. Lett. **96**, 023905 (2006).
[10] P. J. Y. Louis, E. A. Ostrovskaya, C. M. Savage, and Y. S. Kivshar, Phys. Rev. A **67**, 013602 (2003).
[11] D. E. Pelinovsky, A. A. Sukhorukov, and Y. S. Kivshar, Phys. Rev. E **70**, 036618 (2004).
[12] A. A. Zozulya and D. Z. Anderson, Phys. Rev. A **51**, 1520 (1995).
[13] N. G. Vakhitov and A. A. Kolokolov, Radiophys. Quantum Electron. **16**, 783 (1973).
[14] C. Farrell and U. Leonhardt, J. Opt. B: Quantum Semiclassical Opt. **7**, 1 (2005).